

Supporting information

Fluoride doped SrTiO₃/TiO₂ nanotube arrays with double layer walled structure for enhanced photocatalytic property and bioactivity

Chaorui Xue^{a*}, Shengliang Hu^a, Qing Chang^a, Ying Li^a, Xi Liu^a, Jinlong Yang^{a,b}

^aSchool of Materials Science and Engineering, North University of China, Taiyuan 030051, P. R. China

^bSchool of Materials Science and Engineering, Tsinghua University, Beijing 100084, P. R. China

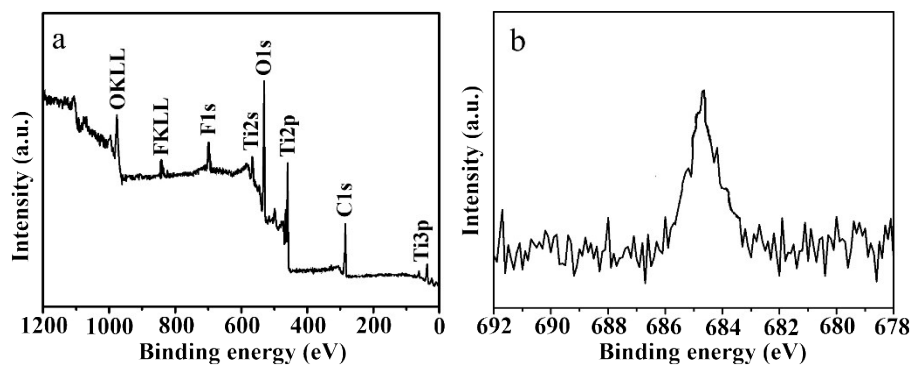


Fig. S1 (a) wide scanning and (b) high resolution F1s XPS spectra of as anodized double layer walled TiO_2 nanotube array.

Fig. S1 shows the XPS spectra of as anodized double layer walled TiO_2 nanotube array. Fig. S1a is the wide scanning XPS spectra, it indicates that Ti, O, F, C appear in the double layer walled TiO_2 nanotube array. Therefore, during anodization process, fluoride ions can be incorporated inside TiO_2 nanotubes. In Fig. S1b, high resolution XPS spectrum of F1s is shown inside. It is easy to identify a F1s peak at 684.7 eV, which corresponding to the fluoride ions physically adsorbed on the sample surface.

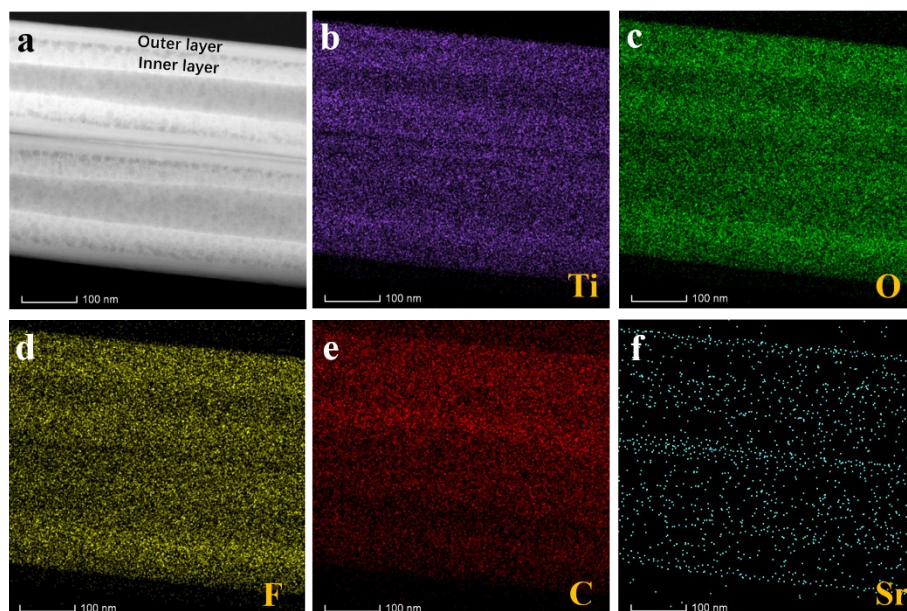


Fig. S2 TEM micrograph and EDX mapping of present elements (Ti, O, F, C, Sr) for TiO_2 nanotubes with hydrothermal treatment in sodium hydroxide solution ($\text{pH} = 12$) containing $0.04 \text{ mol}\cdot\text{L}^{-1}$ strontium acetate inside.

Fig. S2 displays TEM image and EDX elemental mapping for TiO_2 nanotubes with hydrothermal treatment in sodium hydroxide solution ($\text{pH} = 12$) containing 0.04

mol•L⁻¹ strontium acetate inside. The EDX mapping identifies the presence of Ti, O, F, C and Sr in nanotubes. Moreover, Fig. S2f provides the solid proof that the distribution of Sr is not uniform in the nanotubes. The accumulation of Sr in the outer layer of tube wall can be observed clearly.

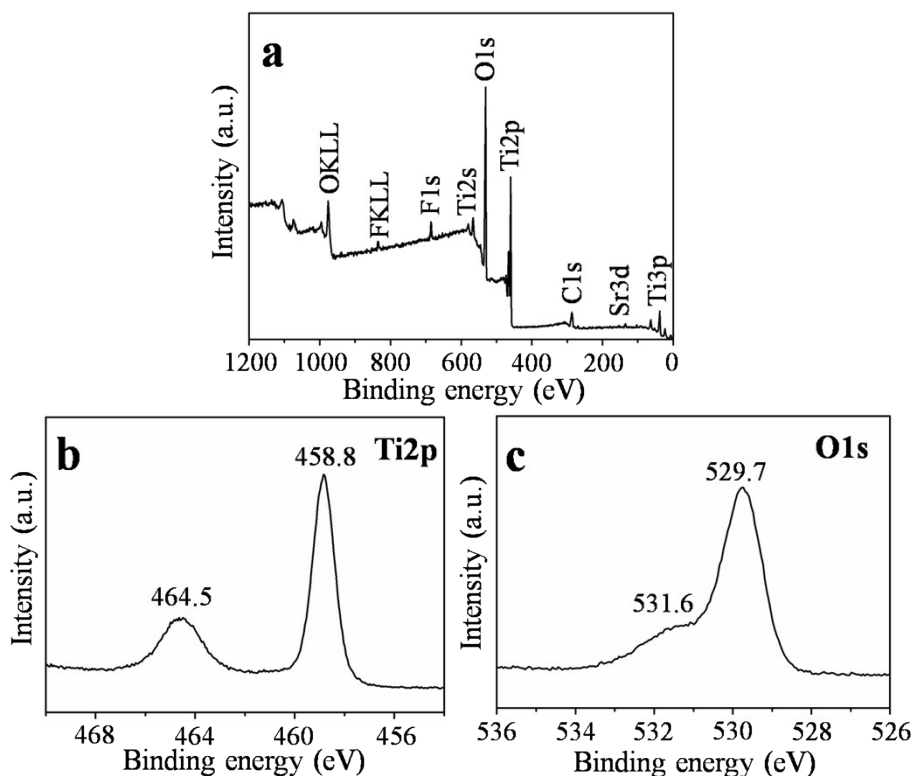


Fig. S3 (a) Wide scanning, (b) high resolution Ti2p and (c) high resolution O1s XPS spectra of annealed double layer walled SrTiO₃/TiO₂ nanotube arrays.

Fig. S3 shows the XPS spectra of annealed double layer walled SrTiO₃/TiO₂ nanotube arrays. Clearly, the full spectrum of Fig. S3a demonstrate that Ti, O, Sr and F elements are existent in the sample. The peak of Sr and F suggests the incorporation of strontium and fluoride. Fig. S3b show the Ti2p spectrum. It is seen that the binding energy of Ti2p_{3/2} is equal to 458.8 eV and the binding energy of Ti2p_{1/2} is equal to 464.5 eV. According to reference 1, titanium exists as 4+ state. In the O1s spectrum of Fig. S3c, two peaks appeared and centered at 529.7 eV and 531.6 eV. The first peak corresponds to the oxygen atoms bound to Ti and Sr. The second peak originates from hydroxyl groups.

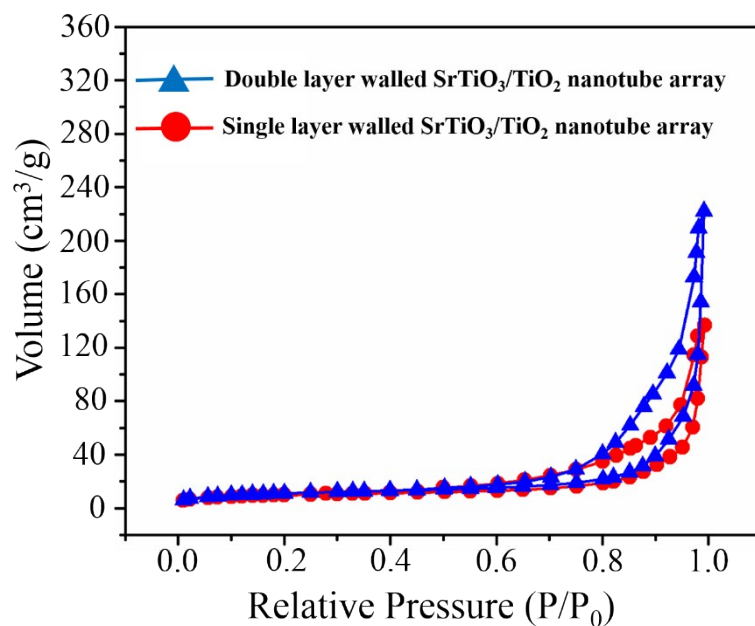


Fig. S4 BET adsorption-desorption isotherm of single and double layer walled SrTiO₃/TiO₂ nanotube arrays.

Fig. S4 demonstrates the nitrogen adsorption-desorption isotherms of both single and double layer walled SrTiO₃/TiO₂ nanotubes. The BET surface area of double layer walled SrTiO₃/TiO₂ nanotubes is 37.77 m²•g⁻¹, which is higher than that of single layer walled SrTiO₃/TiO₂ nanotubes (32.74 m²•g⁻¹).

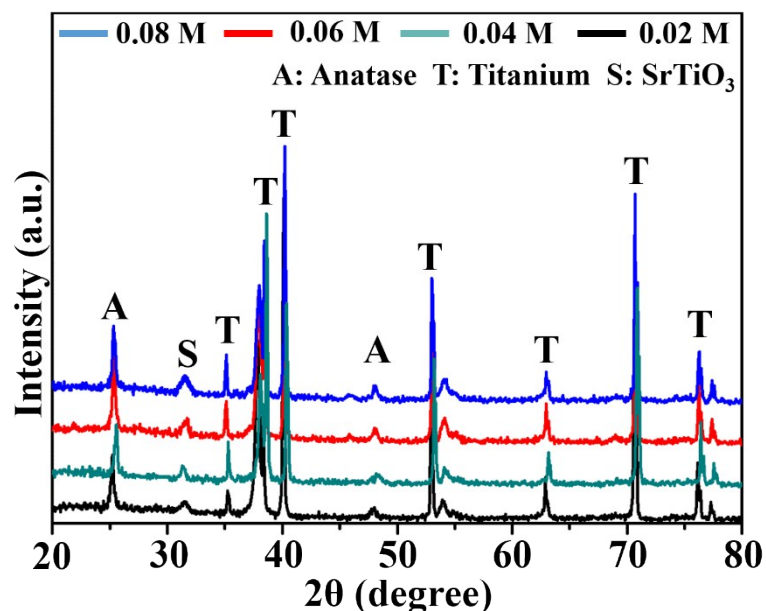


Fig. S5 XRD patterns of double layer walled SrTiO₃/TiO₂ nanotube arrays prepared by hydrothermal treatment in sodium hydroxide solution (pH = 12) with 0.02, 0.04, 0.06 and 0.08 mol•L⁻¹ strontium acetate inside.

Fig. S5 shows the diffraction patterns for double layer walled SrTiO₃/TiO₂ nanotube arrays prepared in sodium hydroxide solution (pH = 12) containing 0.02, 0.04, 0.06 and 0.08 mol•L⁻¹ strontium acetate inside. Characteristic peaks of titanium, anatase and perovskite SrTiO₃ can be observed clearly inside, indicating identical crystalline structure for the double layer walled SrTiO₃/TiO₂ nanotube arrays prepared in all types of solution. Moreover, with the increasing concentration of strontium acetate, peak intensity of perovskite SrTiO₃ become higher. The reason could be larger amount of SrTiO₃ were formed during hydrothermal treatment in solution with higher concentration of strontium acetate.

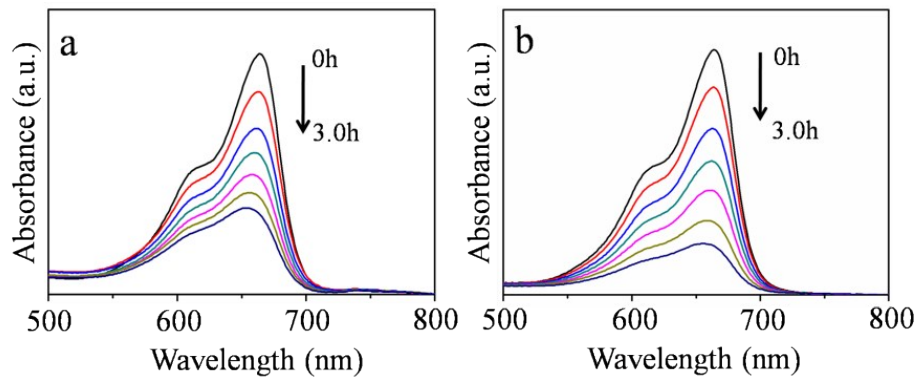


Fig. S6 UV-Vis absorption spectra of methylene blue solution photo-degraded by (a) single and (b) double layer walled SrTiO₃/TiO₂ nanotube arrays under simulated solar light irradiation.

Fig. S6 shows the UV-Vis spectra of MB solution before and after simulated solar light irradiation for different time in the presence of double and single layer walled SrTiO₃/TiO₂ nanotube arrays. It is obvious that the intensity of characteristic absorption peak at 664 nm decreased gradually with time. This indicates that the MB solution has been successfully degraded by the as prepared samples in our work. One can also note that the double layer walled SrTiO₃/TiO₂ nanotube arrays are more efficient than the single layer walled SrTiO₃/TiO₂ nanotube arrays. It is well known that the decomposition kinetics of MB solution follow essentially a first order kinetics, with classical equation $\ln(c/c_0) = k \times t$, where k is the pseudo-first order kinetic rate constant and t is the time². The c/c_0 , which is regarded as the time-dependent

normalized dye concentration, can be calculated by measuring the intensity of characteristic peak at 664 nm. Therefore, Pseudo-first-order kinetic rate plots of the photocatalytic degradation of MB solution for the four samples were obtained and shown in Fig. 6.

References

- 1 D. Li, H. Haneda, S. Hishita and N. Ohashi, *Chem. Mater.*, 2005, **17**, 2596-2602.
- 2 R. Hahn, M. Stark, M. S. Killian and P. Schmuki, *Catal. Sci. Technol.*, 2013, **3**, 1765-1770.